# Optical and Electrical properties of CeO2-P2O5 glasses

**Fawzia zaid, Alhakimah Aleshi.**
**Faculty of Education University of Zawia**

## Abstract:

The study examines the electrical and optical properties of $xCeO_2\cdot(100–x)\ P_2O_5$ glasses, revealing a positive correlation between their electrical conductivity and cerium oxide content. Higher $CeO_2$ concentrations increase conductivity and activation energy decrease. While the glasses exhibit semiconducting behavior due to the electron hopping mechanism between cerium ions between $Ce^{4+}$ and $Ce^{3+}$ ions. UV-Absorption-Spectroscopy was used to analyze the optical properties. UV absorption spectra are due to both $Ce^{3+}$ ions that due to from the 4f±5d transformations and also $Ce^{4+}$ that are attributed to charge transfer ($O^{2+} \rightarrow Ce^{4+}$). Finding that the energy gap and Urbach-Energy decrease with increased $CeO_2$ content up to 40 mol%. This understanding of the composition of cerium phosphate glass could lead to improved material design for future applications, such as potential application as materials for magneto-optical devices.

**Keywords:** *Composition Glass, melting Glass, Absorption, conductivity, Optical band gap.*

## الملخص:

تتناول الدراسة الخصائص الكهربائية والبصرية لنظائر زجاجية من $xCeO_2\cdot(100–x)P_2O_5$ كاشفة عن وجود ترابط إيجابي بين موصليتها الكهربائية ومحتوى أكسيد السيريوم. تزيد الموصيلية بزيادة تركيزاكسيد السيريوم، وتقل طاقة التفعيل، و تظهر النظائر سلوكًا شبه موصل نتيجة لآلية الانتقال الإلكتروني بين أيونات السيريوم $Ce^{4+}$ و $Ce^{3+}$ . لقد تم استخدام طيف امتصاص الأشعة فوق البنفسجية لتحليل الخصائص البصرية. وتعزى اطياف امتصاص الأشعة فوق البنفسجية إما إلى أيونات $ce^{3+}$ الناتجة عن تحويلات $4f \pm 5d$ وأيضًا $ce^{4+}$ التي يمكن أن تُعزى إلى نقل الشحنة $(O^{2+} \rightarrow ce^{4+})$. وجد أن فجوة الطاقة وطاقة اورباخ تتضاءل مع زيادة محتوى $CeO_2$ حتى 40 % مول، قد يؤدي

# Optical and Electrical properties of $CeO_2$-$P_2O_5$ glasses

Fawzia zaid, Alhakimah Aleshi.

هذا التحليل الى فهم تركيب زجاج فوسفات السيريوم وإلى تحسين تصميم المواد لتطبيقات مستقبلية، مثل التطبيق المحتمل كمواد للأجهزة المغناطيسية البصرية.

1. **Introduction:** Nowadays, conducting glass based modern potential applications in certain optical devices becomes a part of large interest. Due to this, conducting glass is still an important class of materials from the last four decades. It is well known that conducting glass exhibits excellent thermal, chemical, dielectric, mechanical, and biological properties, which make it potent candidate for various modern applications [1, 2, 3]. Studying electrical conductivity, density and optical properties of phosphate glasses is of importance for understanding these materials and their applications [4].

The fact that rare-earth-ions in glass may reside in several valence states means, that glasses containing rare earth oxides are likely to have unique and intriguing features. Cerium dioxide is used in making various types of commercial glasses. In some opthalmic glasses, as for example, Crookes lenses, as much as 10 wt %. $CeO_2$ is added for ultraviolet protection. he presence of cerium ions, particularly cerium (IV), makes the glass completely opaque to near ultraviolet radiations. Since cerium absorption in these glasses has a steep cut-off edge, the visible contribution of cerium is very low and thus almost colourless glasses can be obtained with complete absorption to the ultraviolet [3, 5, 6].

Glasses with cerium oxide included in a phosphate glass network are specific types of rare-earth phosphate glass. Several variables effect their electrical conductivity. Ionic conduction primary mechanism of electrical conduction in these glasses is through the movement of ions, particularly $Ce^{3+}$ and $Ce^{4+}$ ions. The ratio of cerium to phosphate affects conductivity. Higher cerium content generally increases conductivity and $Ce^{3+}$ to $Ce^{4+}$ ions influences conductivity, as $Ce^{3+}$ ions are generally more mobile

Conductivity typically increases with temperature due to increased ion mobility. Structural modifications: The addition of other components or heat treatments can alter the glass structure and affect conductivity [4].

Most of the above-mentioned beneficial properties, imparted by cerium ions in glass, depend critically on their ultraviolet absorption characteristics. It is known that under normal conditions of melting, cerium in glass distributes between $Ce^{3+}$and $Ce^{4+}$; the ratio of these two oxidation states being dependent mainly on the composition of the glass

The occurrence of two valences in the case of cerium ions affects the absorption properties of these ions. The electron donation ability of the lower valent ions facilitates the excitation of an electron from the 4f to the 5d shell. On the other side, the electron acceptance ability of the higher valent ions favours charge transfer (CT) transitions from ligands to the cerium ions. Since 4f±5d and CT absorptions are allowed electronic transitions, they have high intensities and are sensitive to the host glass matrix [7, 8].

## 2. Experiment:

The [$xCeO_2.(100-x)\ P_2O_5$, (x= 10, 20, 30 and 40 mol%)] glasses were prepared by melt-quench technique. Reagent grade $CeO_2$ and $NH_4H_2PO_4$ crystalline powders were used as raw materials. The powders were mixed in the desired proportions and melted in porcelain crucibles at temperatures ranging from 1250˚C to 1320˚C, except the sample containing 40 mol% $CeO_2$, the powder was added part by part to simplify the melting process and the temperature is raised gradually to 1450 ˚C. This processes takes 2 hours form the first addition of the powder in the crucible to obtaining the final melt

The dc conductivity was determined by measuring the resistance in the range of $10^3$– $10^{13}$ Ω. The used device was Keithley High Resistance Meter Model 6517B. Samples were ground to obtain parallel-sided disks with a thickness ranging between 1.5 and 3 mm, and graphite was used as a coating material. To measure the resistance, one or two samples of each composition were used. About ± 0.04 eV is considered as an experimental error in computing the activation energy; whereas, a relative error in the conductivity is expected to be ± 5%.

The optical properties of the studied glasses and glass–ceramics were investigated by UV–Visible–NIR Spectrophotometer (JASCO model V770) to determine the optical transition in the range 190–2000 nm through absorption spectra with a resolution of 2 nm.

## 3. Result and discussion

**3.1 DC conductivity:** Figure 1 shows the temperature dependence of the conductivity σ of the $xCeO_2\cdot(100–x)P_2O_5$ glasses investigated. The data reveals a linear relationship between the logarithm of conductivity (log σ) and the inverse of temperature multiplied by 1000 (1000/T). This linear correlation suggests that the primary conduction mechanism in the glasses under study is ionic in nature. Typically, ionic conduction is influenced by three main factors: the concentration of cerium ions, the mobility of these ions, and the structural characteristics of the host matrix. The observed linear trend in the log σ versus 1000/T plot aligns with the Arrhenius equation for conduction, which is commonly used to describe temperature-dependent conductivity in materials as follow,

$$\boldsymbol{\sigma = \sigma_0 e^{-E/KT}} \qquad \textbf{( 1)}$$

Here, $\sigma_0$ is a constant. The factors affecting $\sigma_0$ are the thermal history of the glass and its composition. *k*, *T*, *E* are Boltzmann’s constant, the absolute temperature and activation energy for the conduction process, respectively. A marked feature in the plots of Figure is the decrease in the magnitude of the slope of plots with decreasing the temperature. This means that the activation energy for the conduction process is temperature dependent, which is a characteristic feature of conduction.

Figure .2 The variations of activation energy and Log $\sigma_{523}$ (log conductivity at (523 K) with the $CeO_2$ content as shown in Figure .2. It is observed that log$\sigma_{523}$, slight linearly increases and activation energy slight linearly decrease with increasing $CeO_2$ content. The almost change values of ($log\ \sigma_{523}$) indicate that electrical mobility of charge carriers has a significant effect on the conductivity in the matrix as well. When the sample is affect by the external electric field, the movement of charge carriers in the matrix is related to mobility. The latter depends on several factors, such as the state of the paths through which the ions move, as well as the free volume and molar volume of the glass. This was reported in a previous study [7,9].

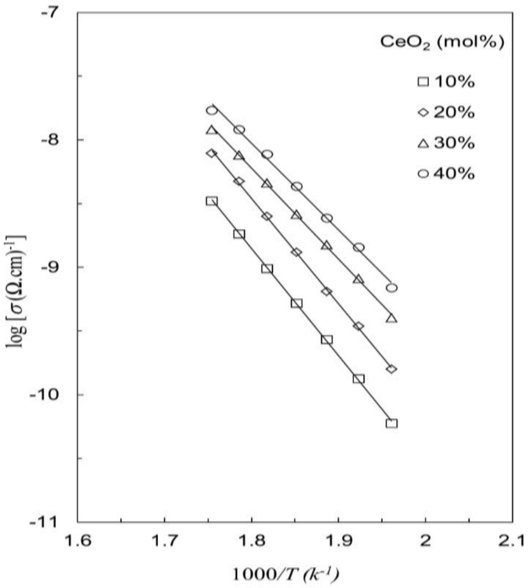

**Fig. 1 Electric conductivity–temperature dependence of$xCeO_2$.(100-x)$P_2O_5$ glasses.**

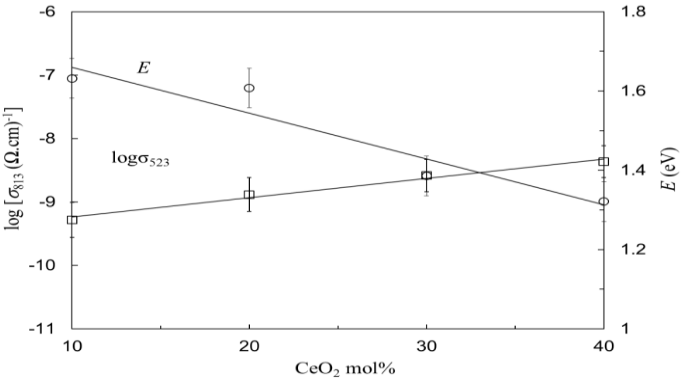

**Fig. 2 The activation energy and the electric conductivity's natural logarithm at T= $523^{o}$K as a function of $CeO_2$ content in $x$$CeO_2$·(100–$x$)$P_2O_5$ glasses . Lines are guides to the eyes.**

The studied glasses are characterized by the presence of $CeO_2$. This oxide may enter the glass structure in the form of Network rate. In addition, cerium ions exist in two forms Such as $Ce^{3+}$ and $Ce^{4+}$. The duality of ionic states allows electrons to jump Back and forth between $Ce^{3+}$ and $Ce^{4+}$ ions. Under external influence. The electric field electrons associated with positive vacancies will jump ion between sites and contribute to the electrical conductivity of the glass. In most species from glass the travel distance is limited and ion. [8].

### *3.2 Optical properties*

Figure. 3 shows the optical absorption spectra of x$CeO_2$·(100–x)$P_2O_5$ glasses as a function of wavelength in the range 190–1100 nm. In order to obtain more information about the structure and properties of the glasses examined, UV-VIS absorption spectra. The spectral curves for four glasses containing varying $CeO_2$ have showed two peaks. The first one appeared at low absorption band around 258 nm which is ascribed to $Ce^{4+}$ ions and the second band around 306 nm is attributed to $Ce^{3+}$ ions. The absorption in UV-VIS region originates from combination absorption from $Ce^{3+}$ is 4f→5d transition and $Ce^{4+}$ is charge transfer ($O^{2+} \rightarrow Ce^{4+}$). The charge transfer band at around

258 nm due to $Ce^{4+}$ is increased and is shifted toward lower wavelengths with splitting by increasing concentration $CeO_2$ due to the structural changes in the glass matrix. This splitting was due to build the bridging bonds around phosphorus atoms, which are constructed P-O-Ce and Ce-O-Ce bonds. Also The charge transfer band was due to oxidation of $Ce^{3+}$ to $Ce^{4+}$ ions, which cause the close packing of oxygen atoms around the $Ce^{3+}$ions. Furthermore, the increase of concentration $CeO_2$ was played as modifier, which was created NBOs to cause higher of negative charges around cerium ions, free oxygen atoms $O^{2-}$ are consumed in building clustered species [7]. Study of the absorption edge in the UV region is a useful method to investigate the transition between electronic bands in amorphous and crystalline materials [10]. It is known that in the absorption process, a photon of known energy excites an electron from lower to a higher energy state, corresponding to an absorption edge. It is deduced that [11] a change of oxygen bonding in the glass network changes the characteristic position of absorption edge.

The optical band gap ($E_g$) is described as the simplest way between the valence and conduction band. It also represents the energy of the electron transition between these two bands. There are different types of optical transitions that may occur through these two bands. It can be seen from the figure. 3 that the optical energy gap ($E_g$) of prepared glasses was obtained by extrapolating the curve (line) to axis. The estimated energy gap values are 3.42, 3.39, 2.91, 2.85 eV with the addition of cerium oxide (10, 20, 30, 40 mol%) respectively, by using the absorption spectrum fitting method proposed by Escobar-Alarcon et al. [12] The relationship between F-the Syrian and the Shumilian [13] is as follows:

$$E_g=1240/\lambda(\mathrm{nm}) \qquad (2)$$

Where λ is wavelength. The decrease in gap energy of the studies glasses may be due to the presence of defect state and non-bridging oxygen.

The mathematical formula correlating the optical absorption coefficient ($\alpha$) with the photon energy ($h\upsilon$) was deduced by Davis and Mott [14] as follows:

$$(\alpha h\upsilon)^n = B(h\upsilon - E_g) \qquad (3)$$

where B is a constant called band tailing parameter, hυ is the incident photon energy and n is the index which can have different values, viz. 1/2, 2, 1/3 and 3 corresponding to direct allowed, indirect allowed, direct forbidden and indirect forbidden, respectively. For amorphous materials, the indirect transitions i.e. n = 2 and n = 3 are valid according to the Tauc's relations. The Tauc's plots for n = 1\2 and n = 2 are shown in Figure. 4(a and b), respectively. The value of $E_g$ can be estimated from the above relation by extrapolating the linear region of the curves to zero absorbance.

The absorption coefficient α is estimated from the optical absorbance A through the relation [15],

$$\alpha(cm)^{-1} = 2.303(A/d) \qquad (4)$$

where d is the sample thickness. In Eq. (3), m takes the following values 1/2 and 2 for direct and indirect transition, respectively. Generally, for oxide glasses [16, 17], indirect allowed transitions (n = 2) are valid which result from electromagnetic interaction of photons with electrons present in the valence band.

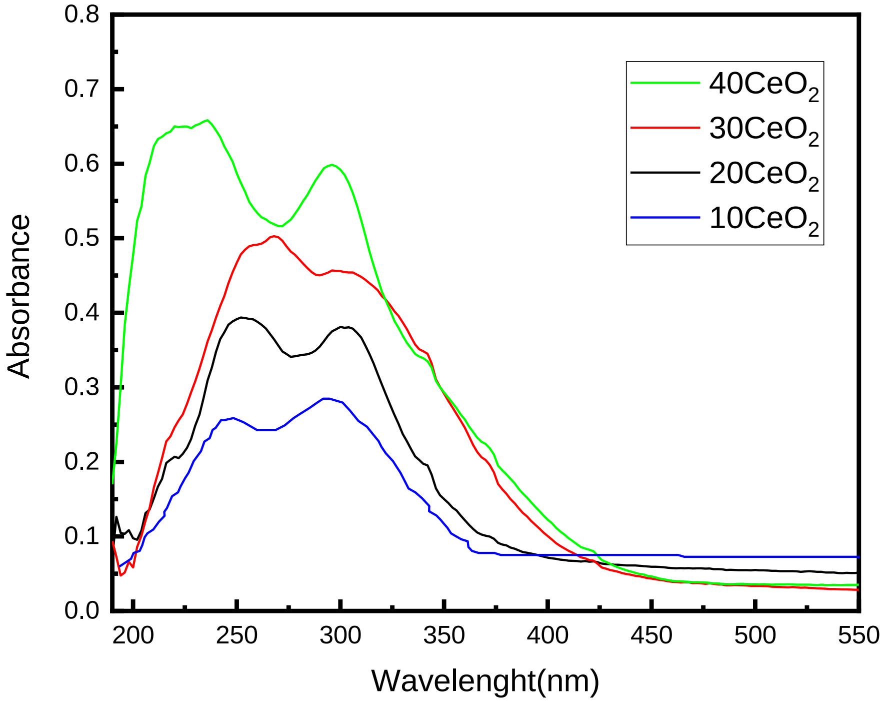

**Fig.3 Absorption spectra of $xCeO_2\cdot(100–x)$ $P_2O_5$glasses**.

The compositional variation of $E_g$ for the two types of transitions (for n = 1/2, n = 2) is shown separately in Figure. 5 and is found to decrease with increasing $CeO_2$ content. These variations in $E_g$ values on addition of $CeO_2$ content can be understood in terms of structural changes occurring in the studied glasses and supports the increase in non-bridging oxygen (NBO) ions. These non-bridging oxygen ions participate to valence band maximum. When a oxygen bond is broken, the bond energy is released and the non-bonding orbitals have higher energies than the bonding orbitals [7]. This suggests that the increase in concentration of NBO ions results in shifting of valence band maximum to higher energies and thus decreases the optical band gap.

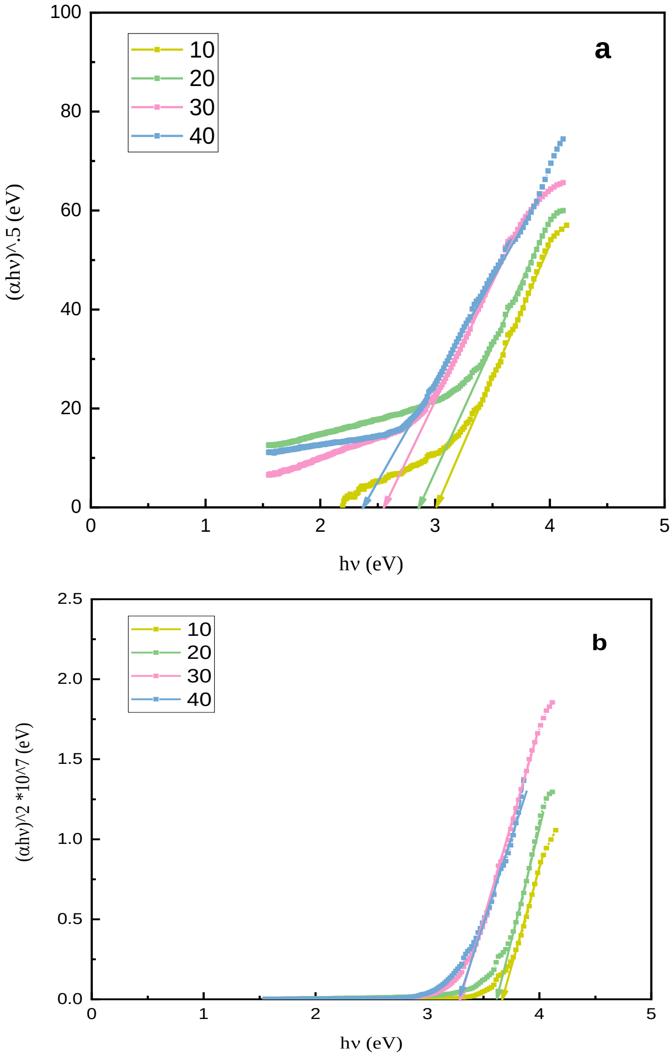

**Fig. 4 Optical gaps as produced by extrapolating the linear parts of the absorptionedge (a) $E_g$ with n= 1/2, (b) $E_g$ with n = 2 for $xCeO_2$-(100-x) $50P_2O_5$ where $CeO_2$ = 10, 20, 30 and 40mol %.**

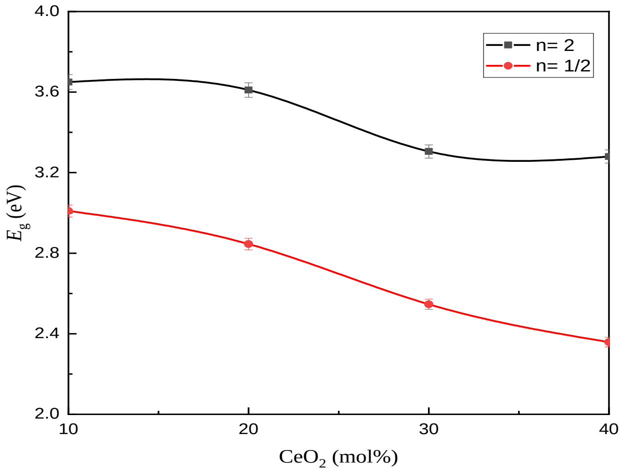

**Fig. 5 Variation of $E_g$ with $CeO_2$ content. the optical band gap $E_g$ for allowed transition for the samples.**

The main feature of the absorption edge of amorphous materials is the dramatic increase in the absorption coefficient with photon energy. When the energy of the incident photon is lower than the band gap, the increase in absorption coefficient is followed by an exponential decay of the density of states localized in the gap [18]. The absorption edge here is called the urbach edge, and it is the energy used to evaluate the quality of a semiconductor.

Figure. 6 shows experimentally plot for ln(α) against photon energy, E = hυ, for determination of the Urbach energy. The following empirical relation gives the Urbach energy and the exponential Absorption tails.

$$\alpha(v) = \alpha_0 e^{hv/E_U} \qquad (5)$$

Here $E_U$ is the Urbach energy which indicates the width of the band tails of the localized states, $\alpha_o$ is a constant. The Urbach energy is calculated by taking the reciprocals of the slope of the linear portion in the lower photon energy of these curves [19].

Figure 7 shows the variation of $E_U$ with $CeO_2$ content. We find that the urbach value decreases with increasing ($CeO_2$) content in the matrix because the number of energy levels in the gap energy decreases and thus the urbach energy decreases. This means that the optical behavior of the urbach energy value is the opposite of the optical behavior. $E_U$ values drop from 1.85 to 0.96 eV. These values are in the range of amorphous semiconductors [20] and may be because long-range ordering can occur locally from the formation of nanoparticle crystalline phases bound to $CeO_2$ as inferred from TEM micrographs [7, 9]. meaning that a sample with a smaller band gap is expected to have a wider band. The activation energy, which defines the disorder associated with one band but not both, should not be confused with the Urbach energy. According to the predicted Urbach energies, which are on the lower limits of the known values for oxide glasses, the electronic defects in this case, the charge-carrying ionic are strongly localized [21].

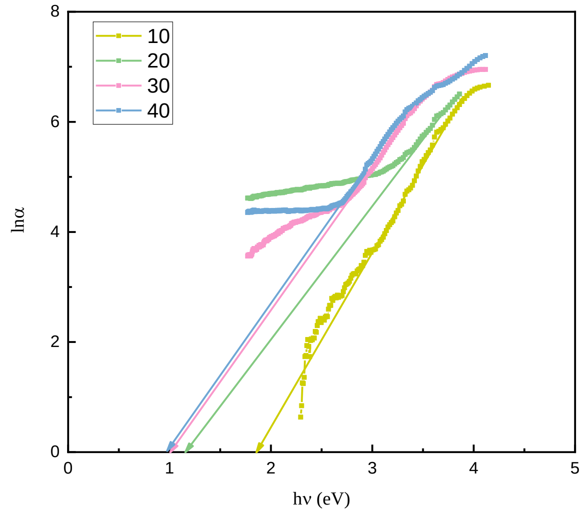

**Fig . 6 Logarithm of the absorption coefficient, ln(α), against photon energy, hυ in $xCeO_2·(100–x)P_2O_5$ glasses .**

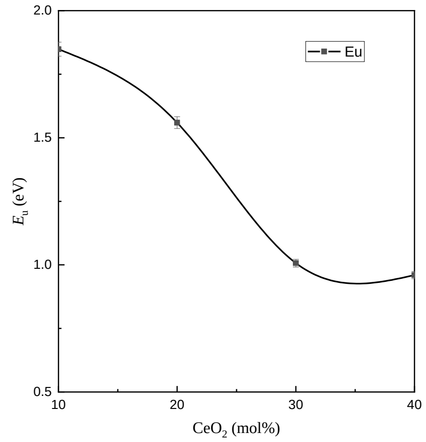

**Fig. 7 Dependence of the Urbach energy $E_U$ on $CeO_2$ content in $xCeO_2 \cdot (100–x)\ P_2O_5$ glasses**

## 4. Conclusion

In oxide glasses, under normal melting conditions, cerium dissociates in trivalent and tetravalent states. The continuous conduction property of the prepared glasses was studied. Optical parameters were calculated from properties measured with UV-Spectroscopy, such as the optical band gap and Uerbach energy. Ionic conduction is the dominant in cerium glasses. It has been suggested that the main source of ionic conduction is the transition between the two valence states of cerium ($Ce^{3+}$ and $Ce^{4+}$). We notice that the activation energy decreases and this increases the ionic conductivity. $E_U$ and $E_g$ decrease with increasing $CeO_2$. These trends are due to the structural changes that occur with the modification of the lattice by $CeO_2$. These observations provide a new avenue for optically transparent ionic conductive glasses that rely heavily on cerium addition formulations.

## Reference:

[1] Blanc, W., Choi, Y.G., Zhang, X., Nalin, M., Richardson, K.A., Righini, G.C., Ferrari, M., Jha, A., Massera, J., Jiang, S. and

Ballato, J., 2023. The past, present and future of photonic glasses: A review in homage to the United Nations International Year of glass 2022. Progress in Materials Science, 134, p.101084.

[2] Sarumaha, C.S., Rajagukguk, J., Chanthima, N., Kidkhunthod, P., Chanlek, N., Kantuptim, P., Yanagida, T., Kim, H.J. and Kaewkhao, J., 2023. Luminescence characteristics of $Ce^{3+}$ doped multicomponent lithium fluorophosphate glasses. Radiation Physics and Chemistry, 207, p.110814.

[3] Kozlova, T.O., Vasilyeva, D.N., Kozlov, D.A., Kolesnik, I.V., Teplonogova, M.A., Tronev, I.V., Sheichenko, E.D., Protsenko, M.R., Kolmanovich, D.D., Ivanova, O.S. and Baranchikov, A.E., 2024. A Comparative Study of Cerium (III) and Cerium (IV) Phosphates for Sunscreens. Molecules, 29(9), p.2157.

[4] Hamdi, M., Shuheil, M.A. and Oueslati, A., 2024. Synthesis, morphological, and ionic conductivity of a lithium cerium diphosphate compound. *Ionics*, pp.1-13.

[5] Barde, R.V., 2016. Influence of $CeO_2$ content on complex optical parameters of phosphovanadate glass system. *Spectrochimica Acta Part A: Molecular and Biomolecular Spectroscopy*, *153*, pp.160-164.

[6] Xia, Y., Calahoo, C., Rodrigues, B.P., Griebenow, K., Graewe, L. and Wondraczek, L., 2023. Structure and properties of cerium phosphate and silicophosphate glasses. *Journal of the American Ceramic Society*, *106*(5), pp.2808-2819.

[7] Gjam, F.Z., Eldamrawi, G., Meikhail, M.S. and Abdelghany, M., 2021. Improving structure and properties of lead phosphate glass through precipitation of few crystals from $CeO_2$. *Egyptian Journal of Chemistry*, *64*(7), pp.3927-3933.

[8] Xia, Y., Calahoo, C., Rodrigues, B.P., Griebenow, K., Graewe, L. and Wondraczek, L., 2023. Structure and properties of cerium phosphate and silicophosphate glasses. Journal of the American Ceramic Society, 106(5), pp.2808-2819.

[9] El-Damrawi, G., Gharghar, F. and Ramadan, R.M., 2016. Structural studies on new $xCeO_2·(50− x) PbO· 50B_2O_3$ glasses and glass ceramics. Journal of Non-Crystalline Solids, 452, pp.291-296.

[10] Alsaif, N.A., Alfryyan, N., Al-Ghamdi, H., Abdelghany, A.M., Sadeq, M.S., Abouhaswa, A.S., Alanazi, A.M. and Rammah, Y.S., 2024. Development of $CeO_2$-doped borophosphate glasses: fabrication, structure and linear/nonlinear optical characteristics for optical purposes. Optical and Quantum Electronics, 56(6), pp.1-15.

[11] Fox, M., 2010. *Optical properties of solids* (Vol. 3). Oxford university press.

[12] Escobar-Alarcón, L., Arrieta, A., Camps, E., Muhl, S., Rodil, S. and Vigueras-Santiago, E., 2007. An alternative procedure for the determination of the optical band gap and thickness of amorphous carbon nitride thin films. *Applied surface science*, *254*(1), pp.412-415.

[13] Souri, D. and Shomalian, K., 2009. Band gap determination by absorption spectrum fitting method (ASF) and structural properties of different compositions of $(60− x) V_2O_5–40TeO_2–xSb_2O_3$ glasses. *Journal of Non-Crystalline Solids*, *355*(31-33), pp.1597-1601.

[14] Mott, N.F., Davis, E.A., Electronic Processes in NonCrystalline Materials, 2nd ed., Oxford, UK: Clarendon,1979.

[15] AbuShanab, W.S., Moustafa, E.B., Hammad, A.H., Ramadan, R.M. and Wassel, A.R., 2019. Enhancement the structural, optical and nonlinear optical properties of cadmium phosphate glasses by nickel ions. *Journal of Materials Science: Materials in Electronics, 30*, pp.18058-18064.

[16] Hivrekar, M.M., Sable, D.B., Solunke, M.B. and Jadhav, K.M., 2018. Different property studies with network improvement

of CdO doped alkali borate glass. *Journal of Non-Crystalline Solids*, *491*, pp.14-23.

[17] Marzouk, S.Y., Seoudi, R., Said, D.A. and Mabrouk, M.S., 2013. Linear and non-linear optics and FTIR characteristics of borosilicate glasses doped with gadolinium ions. *Optical Materials*, *35*(12), pp.2077-2084.

[18] Urbach, F., 1953. The long-wavelength edge of photographic sensitivity and of the electronic absorption of solids. *Physical review*, *92*(5), p.1324.

[19] Ahmadi, F., Hussin, R. and Ghoshal, S.K., 2017. Structural and physical properties of Sm^$^{3+}$ Sm$^{3+}$ doped magnesium zinc sulfophosphate glass. *Bulletin of Materials Science*, *40*, pp.1097-1104.

[20] Davis, E.A. and Mott, N., 1970. Conduction in non-crystalline systems V. Conductivity, optical absorption and photoconductivity in amorphous semiconductors. *Philosophical magazine*, *22*(179), pp.0903-0922.

[21] Rayan, D.A., Abdelghany, A.M., Elshourbgy, A., Hammam, M. and Moustafa, S.H., 2024. Impact of Samarium Ions in the Structural and Optical Characteristics of Aluminum-Sodium Phosphate Glasses. *Advances in Basic and Applied Sciences*, *2*(2), pp.20-28.